Supplemental Figure Legends

Supplemental Figure 1

Toso deficiency results in reduced production of inflammatory cytokines by splenic T cells upon influenza infection.

(**A**) Viral titer kinetics in the BAL fluid of WT and Toso$^{-/-}$ (KO) mice infected intranasally with 1000 PFU influenza virus strain A/PR8 (H1N1). day4: *n*=5; day9: *n*=10. (**B-G**) WT and Toso$^{-/-}$ (KO) mice were infected intranasally with 50 PFU influenza virus strain A/PR8 (H1N1) (*n*= 4-6) or control treated. On day 7 post infection splenocytes were restimulated *ex vivo* and number and frequency of TNFα-producing (**B-D**) and IFNγ-producing (**E-G**) CD4$^+$ T cells (**B, E**) and CD8$^+$ T cells (**C, D, F, G**) was quantified by intracellular cytokine staining. (**D, G**) Cells were restimulated with NP366-peptide, an H-2K^b restricted CD8 T cell epitope of influenza A virus nucleoprotein (peptide comprises amino acids 366-374). Each symbol represents an individual mouse; horizontal line indicates the mean (± SEM). * P<0.05; ** P<0.01; Students *t* test. Data are representative for at least 3 independent experiments.

Supplemental Figure 2

Cell type-specific conditional deletion of Toso.

(**A**) PCR genotyping for Toso (upper panel) and Cre-transgene (lower panel). Splenic CD4$^+$ T cells (left panel), and CD19$^+$ B cells (middle panel) were isolated from the indicated mice by positive selection using magnetic-bead purification (Miltenyi Biotec). Right panel shows data for bone marrow-derived dendritic cells (BMDCs). Genomic DNA was isolated from respective cell types and subjected to PCR analysis. Upper panel: PCR primers specifically recognize the wild-type (WT) allele, the floxed Toso allele and the Toso knock-out (KO) allele. Primer sequences: primer#intron7s, 5'-GGCGCTGCAAAATCTGTGGTTATC-3'; primer#intron7as, 5'-GAAATACCTCTCTCACAGAGG-3'; primer#intron3s, 5'-AGCTCTTCTGGAGTCATAGC-3'. Lower panel: primers are specific for the Cre-transgene and additional primers recognize sequences within the unrelated coronin1a gene locus as a loading control. Primer sequences were: Cre-Tg: primer#Cre-sense, 5'-CCAATTTACTGACCGTACACC-3' and primer#Cre-antisense, 5'- TTACGTATATCCTGGCAGCG-3; loading control: primer#coro1aEx3s, 5'-GTCCACACAATGACAATGTC-3' and primer#coro1aEx4as, 5'-GATGCCAACCCTCTTGGTGT-3'. The size of the expected PCR products is indicated. (**B-E**) Flow cytometric histograms showing Toso-surface expression on the indicated immune cell types from mice of the indicated genotype. Cells were stained with either anti-Toso antibody (grey filled and red line) or isotype matched control antibody (dotted lines).

Supplemental Figure 3

Normal influenza-induced T cell cytokine responses upon conditional deletion of Toso in T cells or dendritic cells.

Mice were infected intranasally with 1000 PFU influenza virus strain A/PR8 (H1N1). (**A-D**) CD4-Cre$^{+/-}$ and Toso$^{f/f}$/CD4-Cre$^{+/-}$ mice (*n*= 6-7), (**E-H**) CD11c-Cre$^{+/-}$ and Toso$^{f/f}$/CD11c-Cre$^{+/-}$

mice (*n*=5). On day 9 post infection lung cells were isolated and restimulated *ex vivo*. Number and frequency of IFNγ-producing (**A, B, E, F**) and TNFα-producing (**C, D, G, H**) $CD4^+$ T cells (**A, C, E, G**) and $CD8^+$ T cells (**B, D, F, H**) was quantified by intracellular cytokine staining. Each symbol represents an individual mouse; horizontal line indicates the mean (± SEM). *n.s.,* not significant; Students *t* test. Data are representative for at least 2 independent experiments.

Supplemental Figure 4

Enhanced expression of PD-1 and PD-L2 in $Toso^{f/f}$/CD19-$Cre^{+/-}$ mice during influenza infection

CD19-$Cre^{+/-}$ mice and $Toso^{f/f}$/CD19-$Cre^{+/-}$ mice were infected intranasally with 50 PFU influenza virus strain A/PR8 (H1N1) and spleens were analyzed at day 7 *p.i.*. (**A, B**) Representative flow cytometric analysis showing (**A**) PD-1 staining on CD4-positive splenic T cells and (**B**) PD-L2 staining on CD19-positive splenic B cells.

Supplemental Figure 5

Reduced immunopathology upon conditional deletion of Toso on B cells in a model of chronic bacterial-induced colitis

CD19-$Cre^{+/-}$ mice and $Toso^{f/f}$/CD19-$Cre^{+/-}$ mice were orally infected with *S.* Typhimurium *ΔaroA* at a dose of 3×10^6 bacteria. (**A, B**) On day 7 *p.i.* spleen cells were restimulated *ex vivo* and number and frequency of TNFα-producing (**A**) $CD4^+$ T cells and (**B**) $CD8^+$ T cells was quantified by intracellular cytokine staining. (**C-G**) Pathology score of infected ceca analyzed at day 7 *p.i.* (**C**) Total cecal pathology score and pathology scores of (**D**) lumen, (**E**) surface epithelium, (**F**) mucosa, and (**G**) submucosa. Pathological scores were determined as follows: Lumen. empty [0], necrotic epithelial cells scant [1]; moderate [2]; dense [3], and neutrophils scant [1]; moderate [2]; dense [3]. Surface epithelium. no pathological changes [0]; desquamation, patchy [1] or diffuse [2], ulceration [1]. Mucosa. no pathological changes [0]; crypt abscesses: rare [1], moderate [2], or abundant [3]; inflammatory infiltrate: rare [1], moderate [2], or abundant [3]; lymphocyte aggregates: rare [0], moderate [1], or abundant [2]. Submucosa. no pathological changes [0]; lymphocyte aggregates: rare [0], moderate [1], or abundant [2]; neutrophils: none [0], moderate [1], or abundant [2]; edema: moderate [1], or severe [2]. (**A-G**) Each symbol represents an individual mouse; horizontal line indicates the mean (± SEM). *Salmonella*-infected mice: *n*= 5-6; Students *t*-test. (**H**) Chronic Salmonella infection-associated change in body weight was monitored over time. Data are expressed as percent of initial body weight. Uninfected: *n*= 2-3; *Salmonella*-infected: *n*= 5-6. * $P<0.05$; ** $P<0.01$; *** $P<0.001$; one-way ANOVA and Tukey's post test.

Supplemental Figure 6

Analysis of TNFα-production in Toso-deficient B cells

(**A, B**) Purified B cells form WT and Toso$^{-/-}$ (KO) mice were treated with LPS, αCD40, αIgM or BAFF+IL21 for 24 h, respectively. For the last 5 hours, cells were stimulated with PMA/ionomycin in the presence of brefeldin A (BFA)/monensin and TNFα production was subsequently analyzed by intracellular cytokine staining. (**A**) Representative flow cytometric analysis of LPS-treated B cells (**B**) Bar graph shows frequency of TNFα-positive B cells. Data are mean ± SEM from 2 cultures derived from different mice. Data are representative for 2 independent experiments.

Supplemental Figure 7

Analysis of Toso-deficient B cells during influenza infection.

WT and Toso$^{-/-}$ (KO) mice were infected intranasally with 50 PFU influenza virus strain A/PR8 (H1N1). On day 14 post infection splenocytes were isolated and analyzed by flow cytometry for frequency and numbers of cells that stained positive for the indicated molecules. (**A**) CD19^{+} B cells; (**B**) GL7^{+}CD95^{+} CD19^{+} B cells; (**C**) CD5^{+} CD19^{+} B cells. (**A-C**) Each symbol represents an individual mouse; horizontal line indicates the mean (± SEM). *n*= 5-6; *n.s.,* not significant; ** *P*<0.01; *** *P*<0.001; Students *t* test. Data are representative for at least 3 independent experiments.

Supplemental Figure 8

Ex vivo characterization of IL-10-producing B cell subsets

(**A**) Purified B cells from IL-10/GFP reporter (Vert-X) mice were treated with BAFF and IL-21 for 16h plus addition of PMA/ionomycin during the last 5 hours. Cells were subsequently stained for the indicated markers and subjected to flow cytometric analysis. Left panel is gated on CD19^{+} B cells and shows staining for B220 vs GFP to identify B2/effector cells (B220^{hi}GFP^{-}), B2/IL-10 cells (B220^{hi}GFP^{+}) and B1/IL-10 cells (B220^{lo}GFP^{+}). Flow cytometric histograms on the right show expression of the indicated surface markers on B2/effector cells (black line), B2/IL-10 cells (blue line) and B1/IL-10 cells (red line). Gray filled: isotype-matched control. (**B, D**) Gating strategy to isolate follicular, marginal zone (MZ) and marginal zone precursor (MZP) B cells from B220^{hi} B cells that, for higher specificity, were negative for NK1.1 and F4/80. Gating was based on expression of either (**B**) IgM, CD21 and CD23 or (**D**) CD1d, IgM and CD23. (**C, E**) Follicular B cells, MZ B cells and MZP B cells were purified by fluorescence activated cell sorting according to the gating strategy shown on the left in (**B**) or (**D**), respectively. Cells were stimulated for 16h with LPS plus PMA/ionomycin/BFA/monensin during the last 5 h and subsequently analyzed for IL-10 production. (**F**) Flow cytometric analysis of naïve B cells from C57BL/6J mice. Left panel is gated on CD19^{+} B cells and shows gating for B220^{hi}CD1d^{-} cells ('B2-CD1d^{-}'), B220^{hi}CD1d^{+} cells ('B2-CD1d^{+}') and B1-B220^{lo} cells. Flow cytometric histograms on the right show expression of the indicated surface markers on B2-CD1d^{-} cells (black line), B2-CD1d^{+} cells (blue line) and B1-B220^{lo} cells (red line). Gray filled: isotype-matched control. Data are representative for at least 3 independent experiments.

Supplemental Figure 9

Phenotypic analysis of IL-10-producing B cells from influenza A-infected mice

IL-10/GFP reporter (Vert-X) mice were infected intranasally with 1000 PFU influenza virus strain A/PR8 (H1N1). Lung and spleen cells were isolated, treated with PMA/ionomycin for 5 hours and subsequently subjected to flow cytometric analysis. (**A**) Lung cells harvested on day 7 *p.i.* were gated on $CD19^+$ B cells. Panel shows staining for B220 vs GFP to identify B2/IL-10-negative cells ($B220^{hi}GFP^-$), B2/IL-10 cells ($B220^{hi}GFP^+$) and B1/IL-10 cells ($B220^{lo}GFP^+$). (**B, C**) B1/IL-10 cells and B2/IL-10 cells in (**B**) lung and (**C**) spleen from infected animals were quantified at the indicated days *p.i.*. Data are expressed as mean ± SEM; symbols represent individual mice; *n*= 3-4. (**D, E**) Flow cytometric analysis of B cells from (**D**) lung and (**E**) spleen harvested on day 7 *p.i.*. Flow cytometric histograms show expression of the indicated surface markers on B2/IL10-negative cells (black line), B2/IL-10 cells (blue line) and B1/IL-10 cells (red line). Gray filled: isotype-matched control.

Supplemental Figure 10

Suppressive function of regulatory B cell subsets is dependent on IL-10

$CD19^+B220^{hi}CD1d^-$ B2 B cells (gray), $CD19^+B220^{hi}CD1d^+$ B2 B cells (blue) and $CD19^+B220^{lo}$ B1a cells (red) were purified from IL-$10^{-/-}$ (KO) mice by fluorescence activated cell sorting and were adoptively transferred into C57BL/6J mice. Mice were infected intranasally with 1000 PFU influenza virus strain A/PR8 (H1N1). On day 9 *p.i.* lung cells were isolated and analyzed for cytokine staining. Number and frequency of TNFα-producing (**A, B**) and IFNγ-producing (**C, D**) $CD4^+$ T cells (**A, C**) and $CD8^+$ T cells (**B, D**). Each symbol represents an individual mouse; horizontal line indicates the mean (± SEM). *n*= 6-7; *n.s.*, not significant; one-way ANOVA and Dunnett's post-hoc test. Data are representative for 2 independent experiments.

Supplemental Figure 11

Normal B cell development in the bone marrow of Toso-deficient mice.

(**A**) Flow cytometric histograms showing Toso surface expression levels on the indicated $CD19^+$ B cell subsets in the spleen. WT (black line); Toso$^{-/-}$ (KO) (gray filled). GeoMFI, geometric mean fluorescence intensity. (**B-G**) Bone marrow cells from WT and Toso$^{-/-}$ (KO) mice were stained with the indicated surface markers and analyzed by flow cytometry. (**B**) Representative FACS profiles in the left panels are gated on $CD19^+$ cells and show staining for CD43 and B220. Right panels are gated on $CD19^+B220^+CD43^-$ cells and show staining for IgM and IgD. (**C**) Toso surface expression on the indicated B cell subsets in the bone marrow. Cells were pre-gated on $CD19^+B220^+CD43^-$ and Toso expression was analyzed on IgM^+IgD^+ mature B (red), IgM^+IgD^- immature B (green), and IgM^-IgD^- pre-B cells (blue). (**D-G**) Frequency and absolute number of the indicated B cell subpopulations in the bone marrow of WT and Toso$^{-/-}$ (KO) mice. Analysis was performed on $CD19^+$ cells (**D**) and $CD19^+B220^+CD43^-$ cells (**E-G**). Data show $B220^+CD43^+$ pro-B cells (**D**), IgM^-IgD^- pre-B cells (**E**), IgM^+IgD^- immature B cells (**F**), and IgM^+IgD^+ mature B cells (**G**). (**D-G**) Each symbol represents an individual mouse; horizontal line indicates the

mean (± SEM); *n*=6; *n.s.,* not significant; Students *t* test. Data are representative for at least 3 independent experiments.

Supplemental Figure 12

Altered development and maturation of splenic B cells in Toso-deficient mice.

Splenocytes from WT and Toso$^{-/-}$ (KO) mice were stained with the indicated surface markers and analyzed by flow cytometry. (**A**) Representative FACS profiles are gated on CD19^{+}B220^{hi} cells and show staining for IgM and IgD. (**B**) CD19^{+}B220^{+} B cells were analyzed for frequency and absolute number of IgM^{hi}IgD^{lo} immature B cells, IgM^{hi}IgD^{hi} transitional B cells, and IgM^{lo}IgD^{hi} mature B cells. (**C**) FACS profiles are gated on CD19^{+}B220^{hi} cells and show staining for CD23 and CD21. (**D**) CD19^{+}B220^{+} B cells were analyzed for frequency and absolute number of CD21^{int}CD23^{hi} follicular B cells and CD21^{hi}CD23^{lo} marginal zone B cells. (**B, D**) *n*=5. (**E**) CD19 and B220 surface levels on spleen cells from WT (gray filled) and Toso$^{-/-}$ (KO) mice (red line). (**F, G**) Surface expression levels of CD21, CD23, IgM and IgD on CD19^{+}B220^{hi} B2 cells from WT and Toso$^{-/-}$ (KO) mice. (**F**) Representative flow cytometric histograms and (**G**) geometric mean fluorescence intensity (GeoMFI; *n*=5) ± SEM are shown. (**H**) Flow cytometric histograms showing representative surface expression levels of the indicated surface receptors on B220^{+}AA4.1^{-}CD1d^{-} B2-effector cells from WT (gray filled) and Toso$^{-/-}$ (KO) mice (red line). Dotted lines show isotype-matched control stainings. Data are representative for at least 3 independent experiments. * P<0.05; ** P<0.01; *** P<0.001; Students *t* test.

Supplemental Figure 13

Splenic and peritoneal B1a B cells are increased in Toso-deficient mice.

(**A, B**) Flow cytometric analysis of splenocytes from WT and Toso$^{-/-}$ (KO) mice. (**A**) FACS profiles are gated on CD19+ cells and show staining for FSC vs. B220. (**B**) Frequency and number of CD19^{+}B220^{lo} B1 B cells and CD19^{+}B220^{hi} B2 B cells in the spleen of WT and Toso$^{-/-}$ (KO) mice. (**C, D**) Peritoneal exudate cells from WT and Toso$^{-/-}$ (KO) mice were stained with the indicated surface markers and analyzed by flow cytometry. (**C**) Left panel: FACS profiles are gated on CD19^{+} cells and show staining for CD19 and B220. Gating for B1 and B2 cells is indicated. Right panel: FACS profiles are gated on B1 cells and show staining for CD43 and CD5. Gating for B1a and B1b cells is indicated. (**D**) Frequency and number of B1 and B2 cells (left panel), and B1a and B1b cells (right panel) in the peritoneal exudate from WT and Toso$^{-/-}$ (KO) mice. Each symbol represents an individual mouse; horizontal line indicates the mean (± SEM). *n.s.,* not significant; * P<0.05; ** P<0.01; *** P<0.001; Students *t* test. (**E**) Peritoneal exudate cells from IL-10/GFP reporter Vert-X mice (right panel) were treated for 5h with LPS and PMA/ionomycin. Cells were stained for CD19, B220, CD5 and CD43 and analyzed by flow cytometry. B2, B1a and B1b subpopulations were identified as shown in (C) and analyzed for GFP expression as a marker for IL-10 production. Cells from normal C57BL/6 mice were treated similarly and served as a negative control (left panel). (**F**) Peritoneal exudate cells form normal WT C57BL/6 mice were treated for 5h with LPS and PMA/ionomycin in the presence of brefeldin A. IL-10 production in B2, B1a and B1b cells was subsequently analyzed by intracellular cytokine staining. (**B, D**) Each symbol represents an individual mouse; horizontal

line indicates the mean (± SEM). (**B**) *n*=5; (**D**) *n*=9. *n.s.,* not significant; * $P<0.05$; ** $P<0.01$; *** $P<0.001$; Students *t* test. Data are representative for at least 3 independent experiments.

Supplemental Figure 14

Self-reactivity of IL-10-competent regulatory B cell subsets.

$B220^{hi}AA4.1^{-}CD1d^{-}$ B2-effector cells, $B220^{hi}CD1d^{+}$ B2-Bregs, $B220^{hi}AA4.1^{+}$ B2-transitional cells (B2-trans) and $B220^{lo}$ B1-Bregs from WT mice were purified by flow cytometric cell sorting and were treated for 3 days with LPS. (**A**) Culture supernatants were analyzed for anti-dsDNA and anti-ssDNA IgM levels (*n*=2). (**B**) Cells were analyzed by flow cytometry for forward scatter (FSC) vs side scatter (SSC) characteristics and CD138 vs CD19 surface expression. Data are representative for at least 2 independent experiments.

Supplemental Figure 15

Altered BCR-responsiveness of Toso-deficient B2-effector B cells.

(**A-D**) $AA4.1^{-}CD1d^{-}$ B2-effector cells, $AA4.1^{+}$ B2-transitional cells, $CD1d^{+}$ B2-Bregs and $B220^{lo}$ B1-Bregs were purified by flow cytometric cell sorting. (**A-B**) High purity sorted B cell subsets from WT (filled bars) and $Toso^{-/-}$ (KO) (hatched bars) mice were stimulated for the indicated times with anti-IgM and analyzed by flow cytometry for (**A**) cell survival and (**B**) cell counts. (**C, D**) High-purity sorted B cell subpopulations from C57BL/6 mice were either cultured with medium (filled bars) or were stimulated with anti-IgM (15 µg/ml; patterned bars). After 24 h cultures were analyzed by flow cytometry for (**C**) cell survival and (**D**) proliferation (cell counts). Data show results for $B220^{hi}AA4.1^{-}CD1d^{-}$ B2-effector cells (dark gray), $B220^{hi}CD1d^{+}$ B2-Bregs (blue), $B220^{hi}AA4^{+}$ B2-transitional cells (green) and $B220^{lo}$ B1-Bregs (red). Data are mean ± SEM from two independent cultures. (**E**) IgM surface expression levels on naïve (=unstimulated) B cell subsets. (**F, G**) Purified $CD19^{+}$ B cells from WT and $Toso^{-/-}$ (KO) mice were treated with (**F**) LPS or (**G**) BAFF plus IL-21. At the indicated times, cultures were analyzed by flow cytometry for cell survival. Data are mean ± SEM from 2 independent cultures. (**H**) Sorted B2-effector cells were stimulated for 16h with titrated concentrations of anti-IgM and analyzed by flow cytometry for upregulation of the B cell activation markers CD25, CD69 and CD86. WT (gray filled); $Toso^{-/-}$ (KO) (red line). Data are representative for at least 3 independent experiments.

Supplemental Figure 16

Toso-expression on human lymphocytes

Flow cytometric analysis of human peripheral blood cells showing surface expression of human Toso on $CD19^{+}$ B cells, $CD4^{+}$ T cells, $CD8^{+}$ T cells and granulocytes. Staining with control IgG (gray filled); anti-human-Toso mAb staining (red line). Anti-human-Toso mAb recognizing the extracellular portion of human Toso was generated by utilizing DNA-immunization of rats. Data are representative for at least 2 independent experiments.

Supplemental Figure 17

Model: Effects of Toso-deficiency on regulatory B cells and T cell immune responses: implications for protective immunity vs immunopathology

Based on our data we propose the following model to explain the immune defects observed in Toso-deficient mice. (**A**) In normal wild type mice the ratio of regulatory B cells (B_{regs}) to effector T cells is tightly balanced, allowing for normal protective T cell immunity. (**B**) Toso-deficiency on B cells leads to increased numbers of B_{regs} that exhibit immunosuppressive activity on effector T cells, resulting in reduced proinflammatory T cell responses. Depending on the type of inflammatory disease and the particular role of T cells in this disease, such suppressed T cell immunity can have different consequences: During acute viral infection (e.g. acute influenza infection), where anti-viral immunity is largely T cell-dependent, impaired T cell responses are detrimental and result in insufficient pathogen clearance and thus defective immune protection. On the other hand, during chronic inflammatory disorders (e.g. chronic *Salmonella*-induced intestinal inflammation), where T cell effector function is more associated with immunopathological tissue damage, higher numbers of B_{regs} and thus reduced T cell effector function is beneficial, as this limits the extend of T cell-mediated tissue destruction. (**C**) High numbers of immunosuppressive B_{regs} (such as e.g. in Toso-deficient mice) are associated with impaired proinflammatory T cell responses and, thus, insufficient anti-viral activity, but provide relative protection from T cell-mediated tissue damage. Conversely, low numbers of B_{regs} are associated with strong proinflammatory T cell responses that provide efficient immune protection against invading pathogens, but on the downside, may also cause immunopathological tissue destruction. In a normal healthy system, B_{reg} numbers are well balanced, thus allowing for pathogen clearance by T cells, while avoiding excessive T cell activation, thus limiting immunopathological tissue damage.

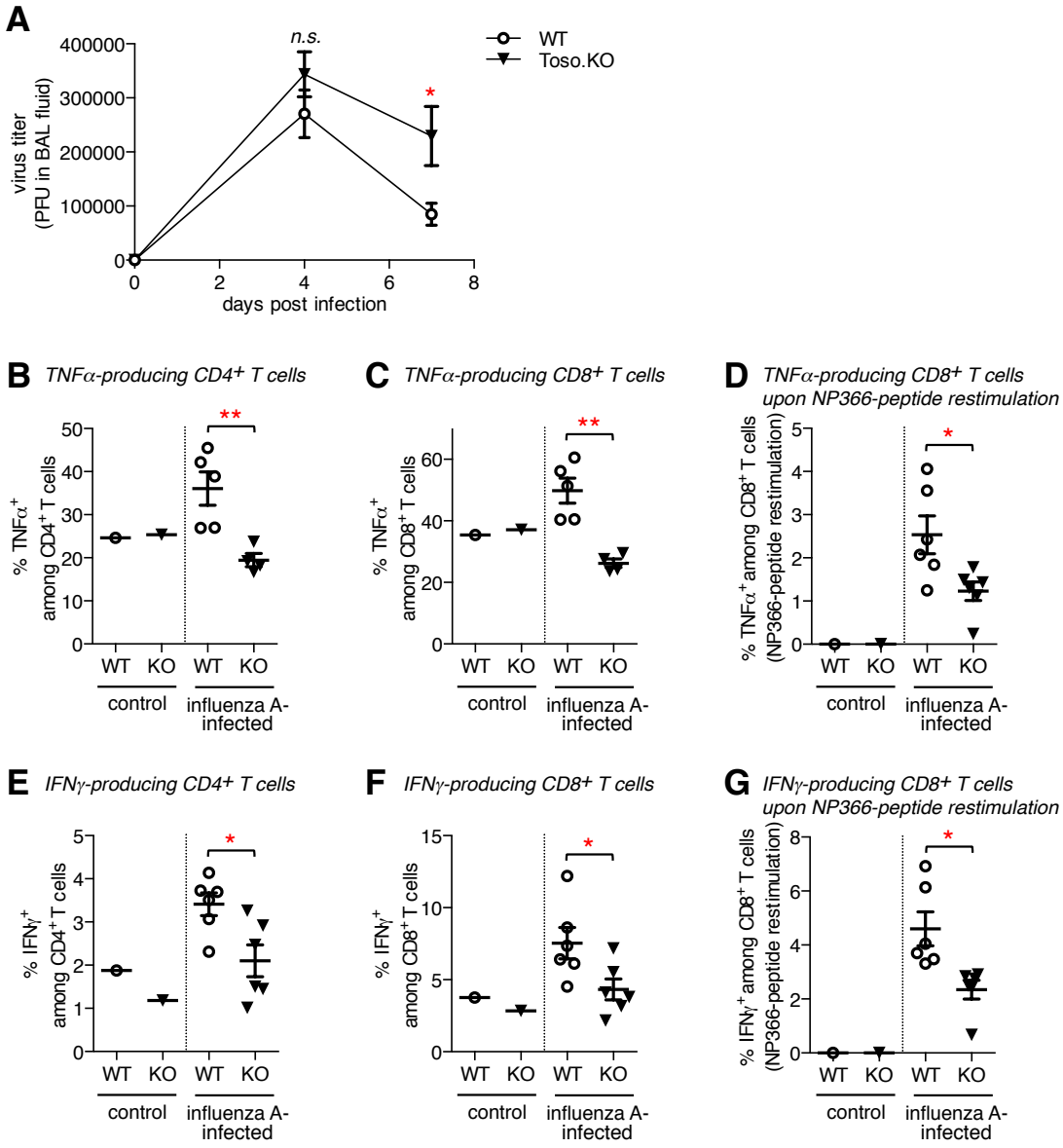

Yu et al., Supplemental Figure 1

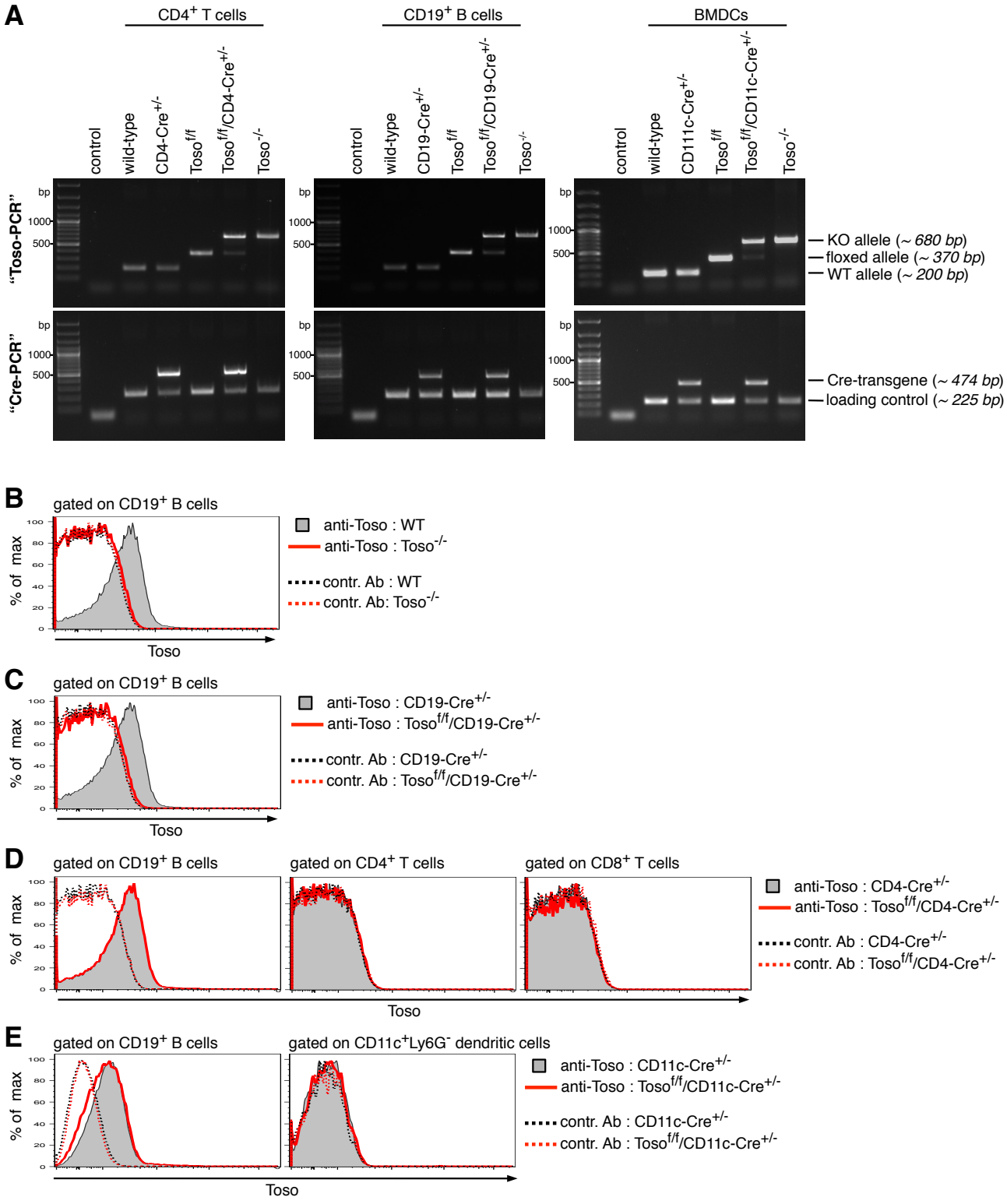

Yu et al., Supplemental Figure 2

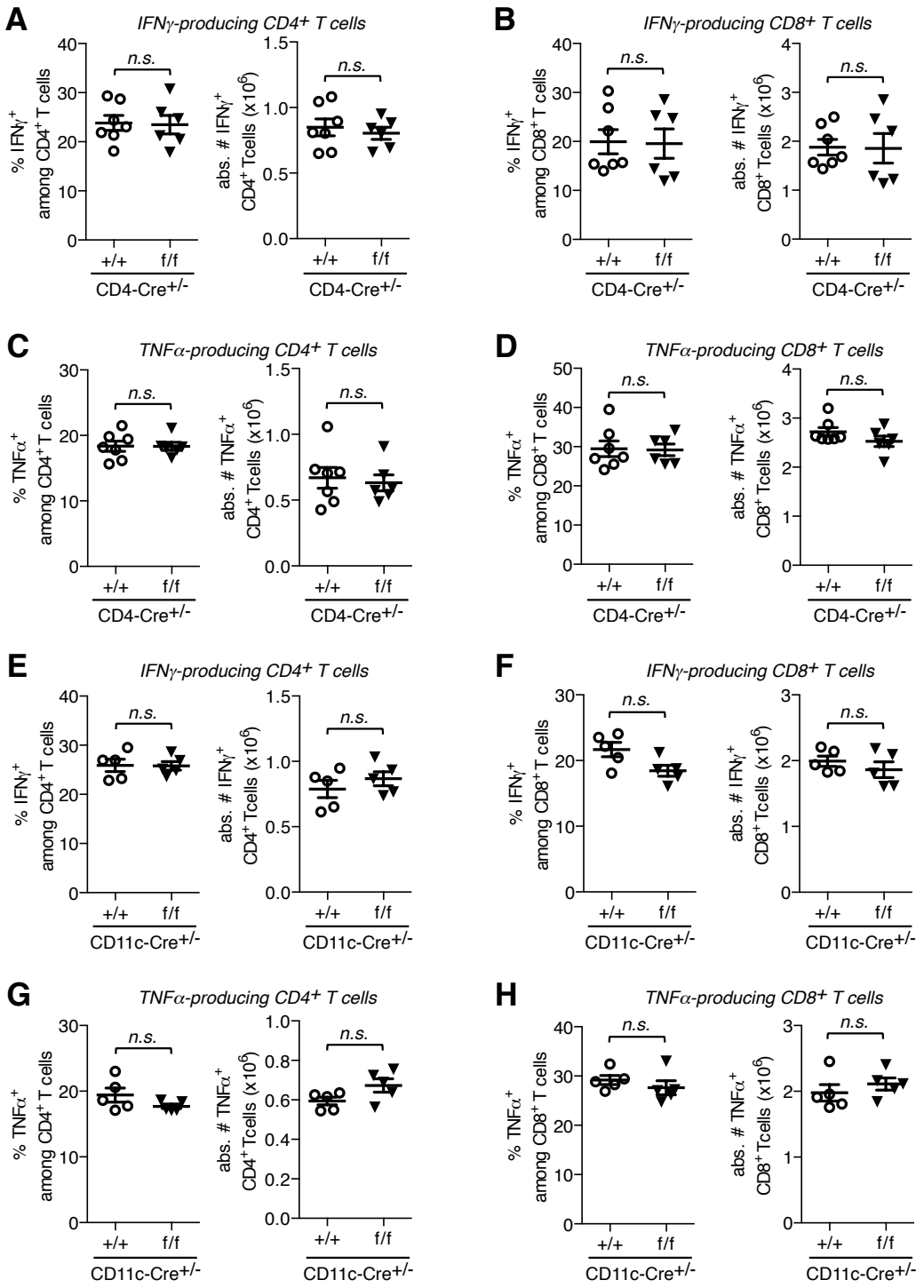

Yu et al., Supplemental Figure 3

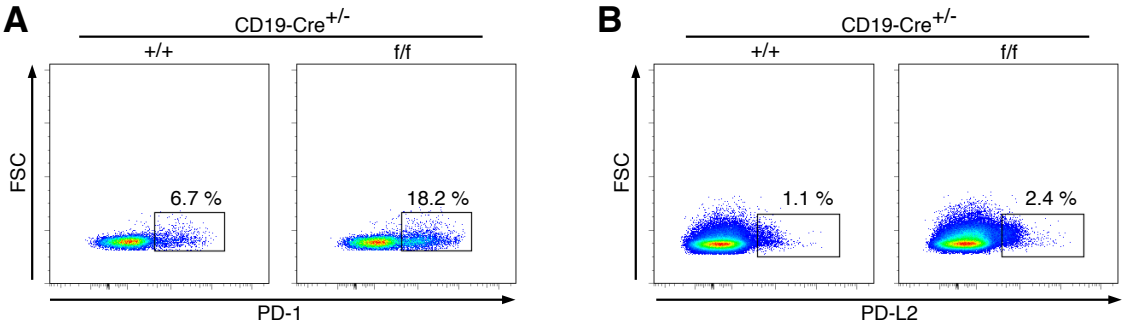
A
CD19-Cre+/-
+/+
f/f
FSC
6.7 %
18.2 %
PD-1
B
CD19-Cre+/-
+/+
f/f
FSC
1.1 %
2.4 %
PD-L2

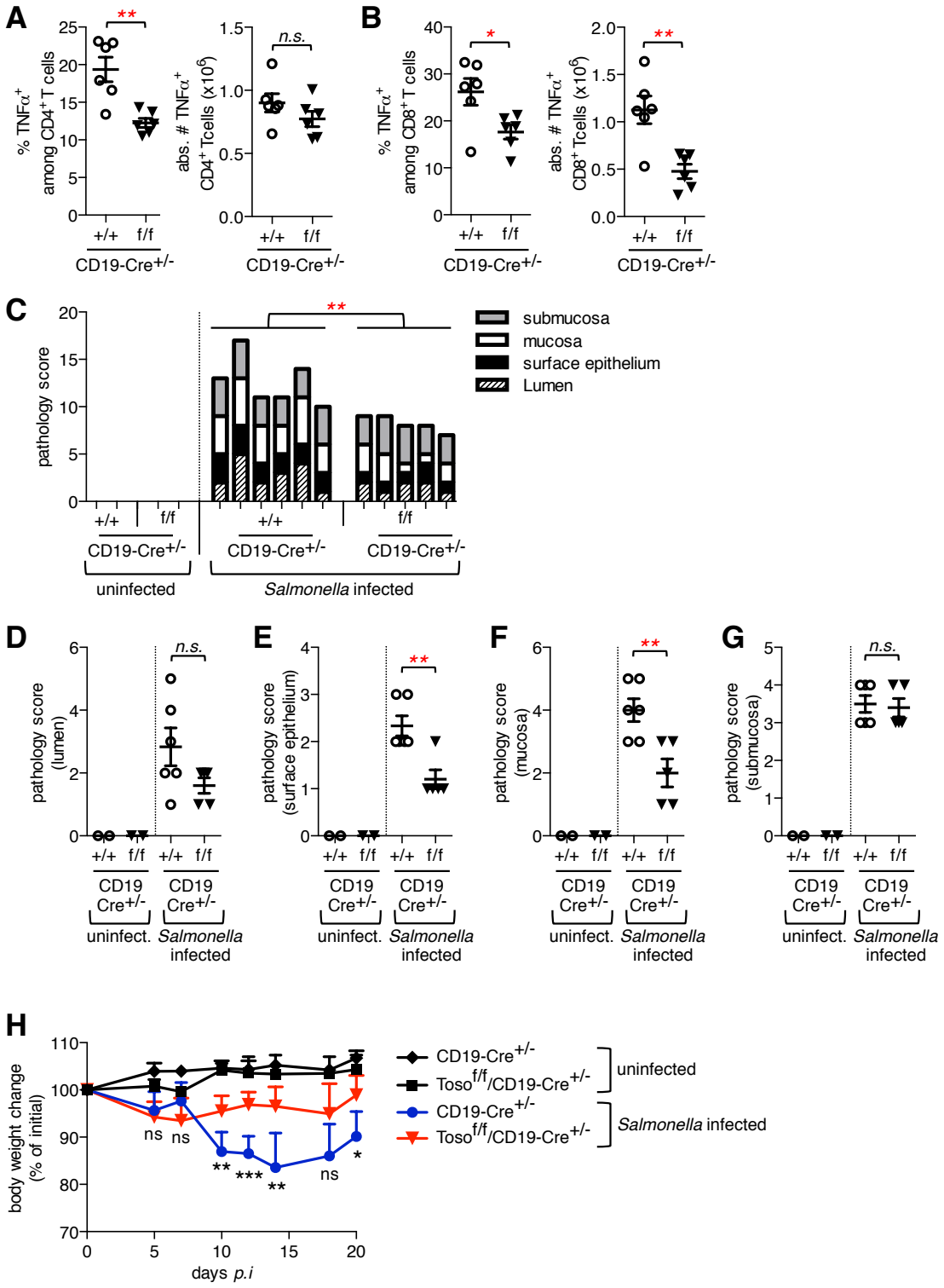
A
% TNFα+ among CD4+ T cells
abs. # TNFα+ CD4+ Tcells (x10^6)
n.s.
B
% TNFα+ among CD8+ T cells
abs. # TNFα+ CD8+ Tcells (x10^6)
+/+
f/f
CD19-Cre+/-
C
pathology score
submucosa
mucosa
surface epithelium
Lumen
uninfected
Salmonella infected
D
pathology score (lumen)
E
pathology score (surface epithelium)
F
pathology score (mucosa)
G
pathology score (submucosa)
CD19 Cre+/-
uninfect.
Salmonella infected
H
body weight change (% of initial)
days p.i
CD19-Cre+/-
Tosof/f/CD19-Cre+/-
uninfected
Salmonella infected
ns

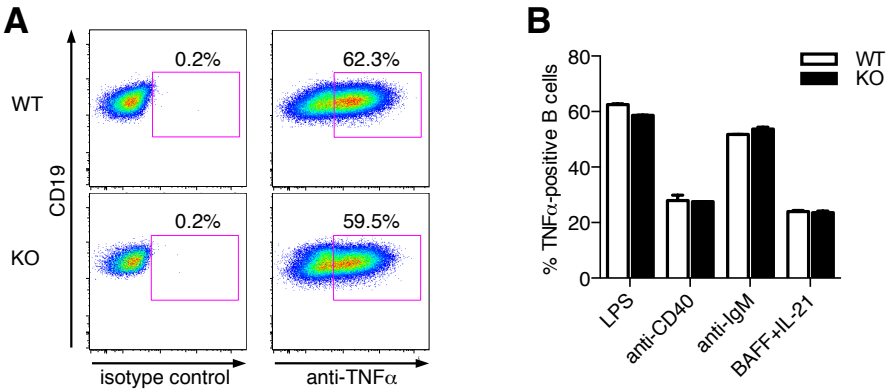
A
WT
KO
CD19
0.2%
62.3%
0.2%
59.5%
isotype control
anti-TNFα
B
% TNFα-positive B cells
80
60
40
20
0
WT
KO
LPS
anti-CD40
anti-IgM
BAFF+IL-21

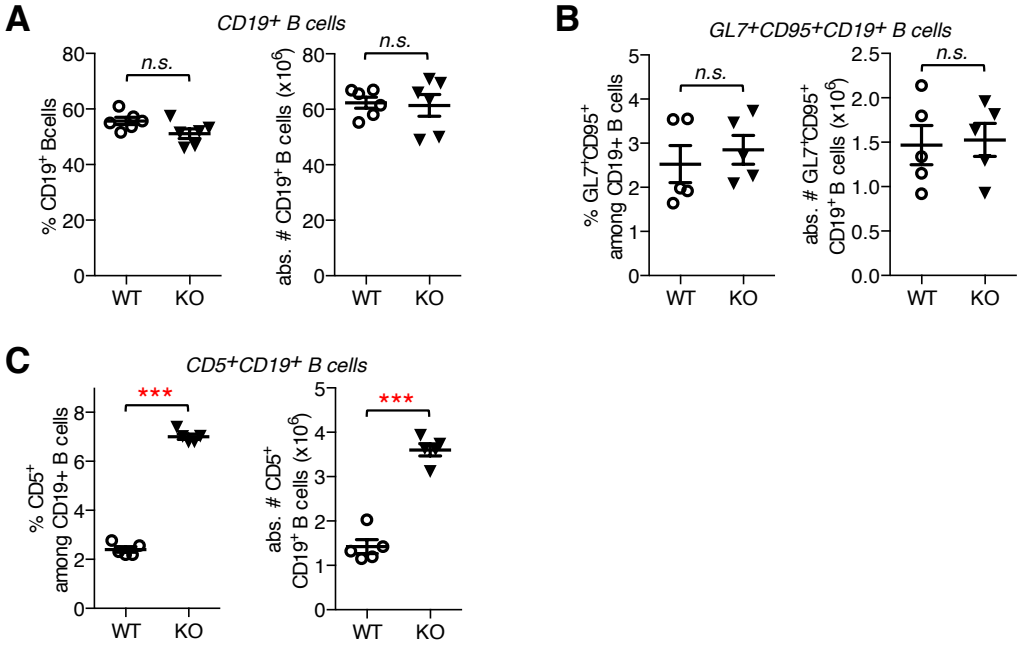

Yu et al., Supplemental Figure 7

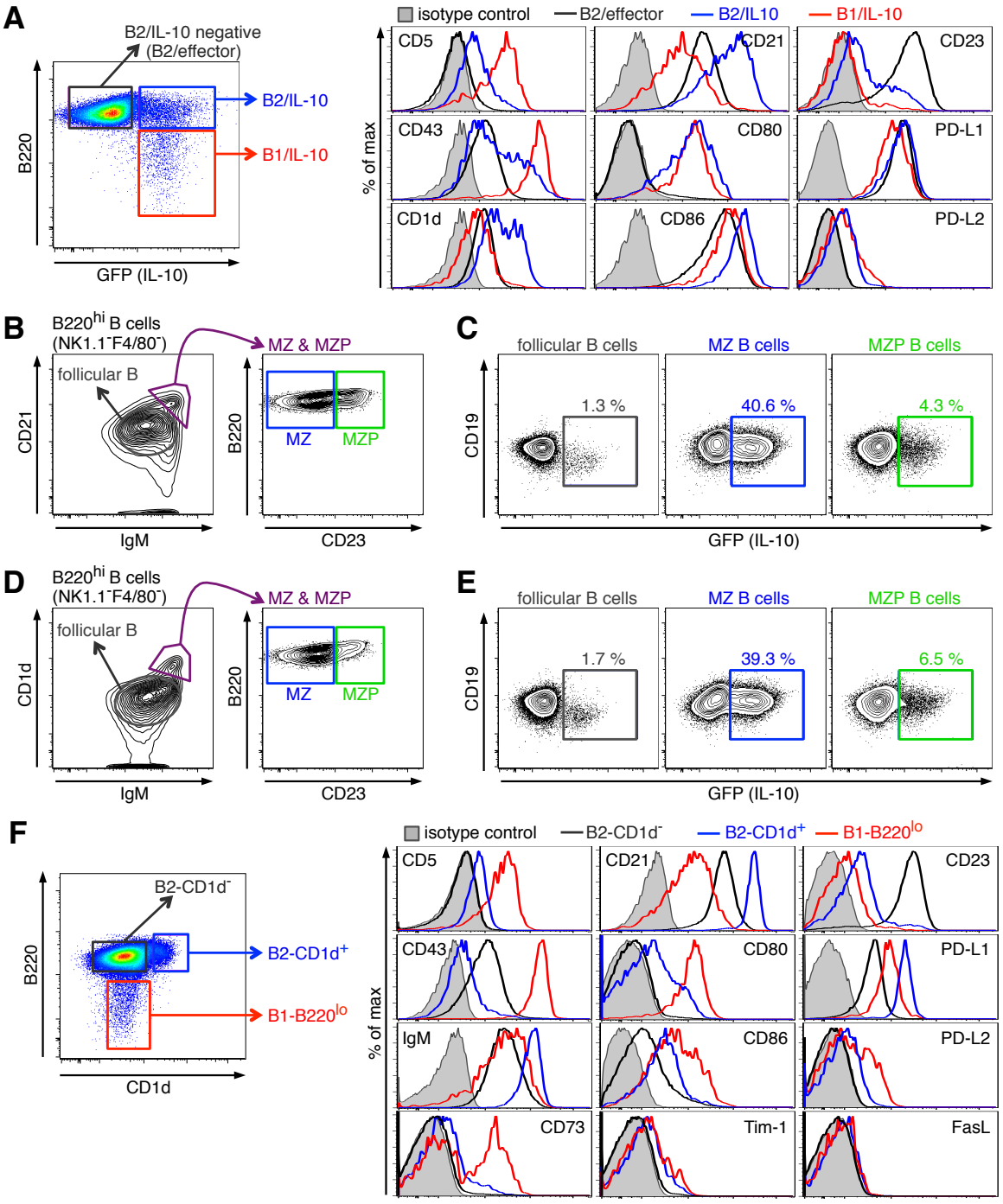

Yu et al., Supplemental Figure 8

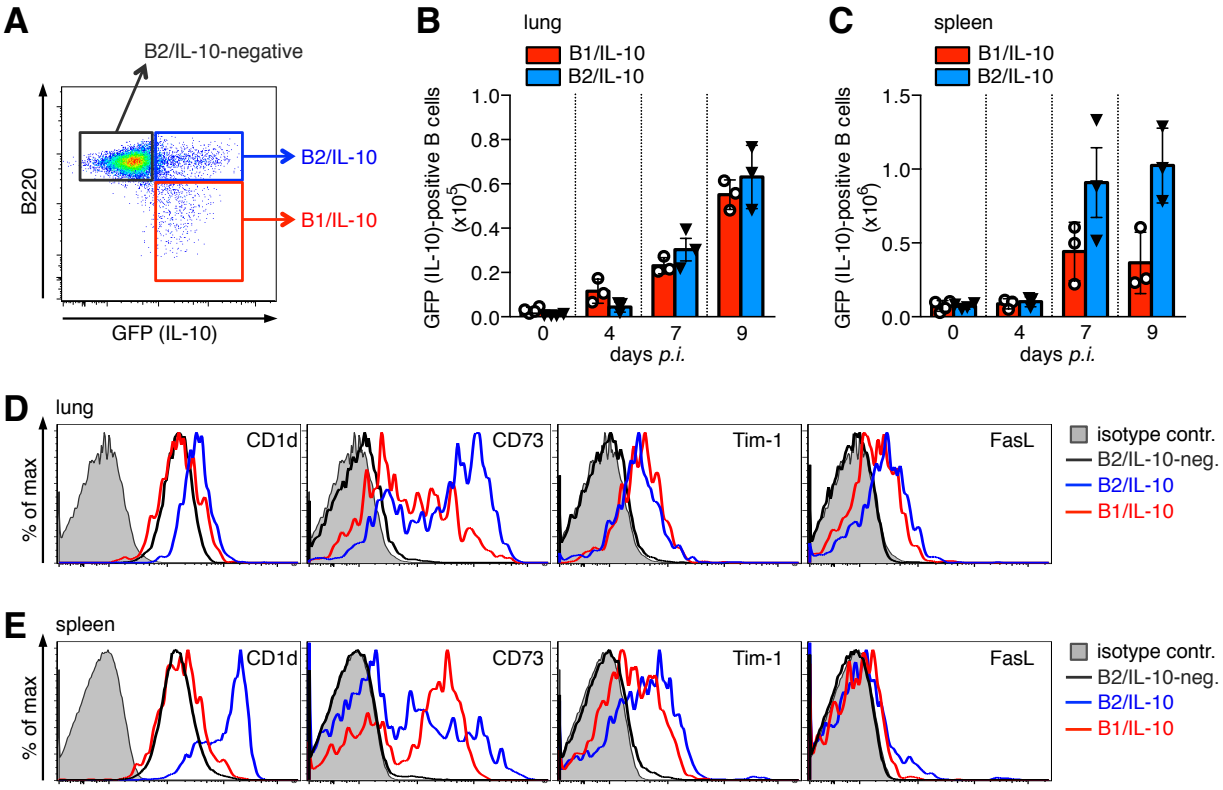

Yu et al., Supplemental Figure 9

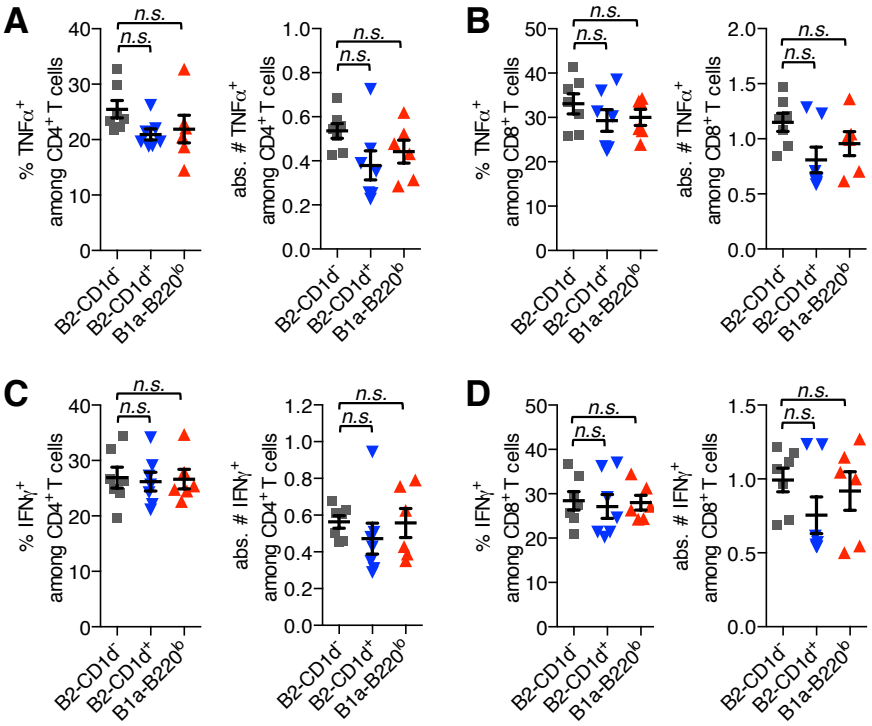

Yu et al., Supplemental Figure 10

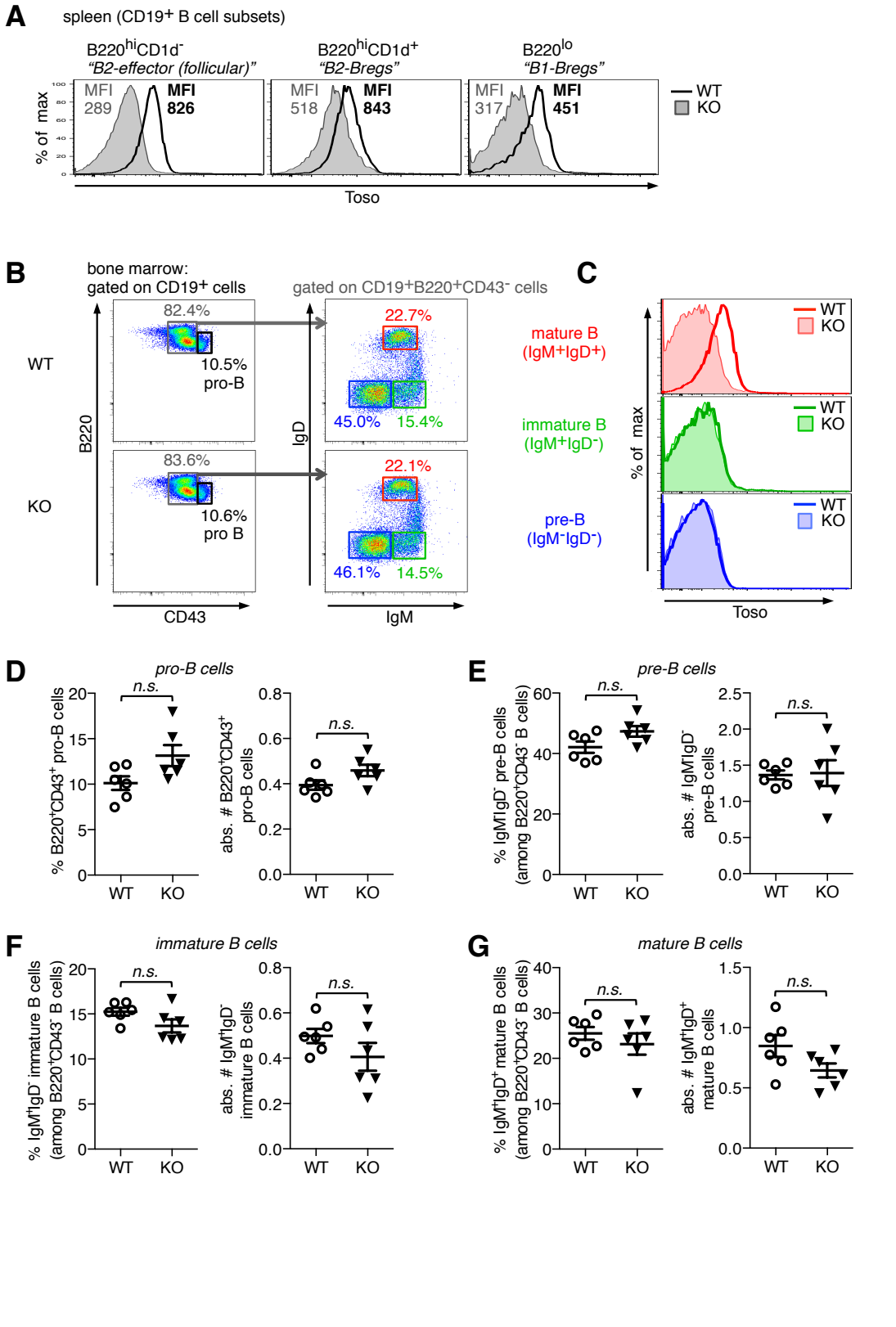
A
spleen (CD19+ B cell subsets)
B220hiCD1d-
"B2-effector (follicular)"
B220hiCD1d+
"B2-Bregs"
B220lo
"B1-Bregs"
MFI 289
MFI 826
MFI 518
MFI 843
MFI 317
MFI 451
% of max
WT
KO
Toso
B
bone marrow:
gated on CD19+ cells
gated on CD19+B220+CD43- cells
WT
KO
82.4%
10.5%
pro-B
83.6%
10.6%
pro B
22.7%
45.0%
15.4%
22.1%
46.1%
14.5%
B220
CD43
IgD
IgM
C
mature B
(IgM+IgD+)
immature B
(IgM+IgD-)
pre-B
(IgM-IgD-)
% of max
Toso
D
pro-B cells
% B220+CD43+ pro-B cells
abs. # B220+CD43+
pro-B cells
n.s.
E
pre-B cells
% IgM+IgD- pre-B cells
(among B220+CD43- B cells)
abs. # IgM+IgD-
pre-B cells
F
immature B cells
% IgM+IgD- immature B cells
(among B220+CD43- B cells)
abs. # IgM+IgD-
immature B cells
G
mature B cells
% IgM+IgD+ mature B cells
(among B220+CD43- B cells)
abs. # IgM+IgD+
mature B cells

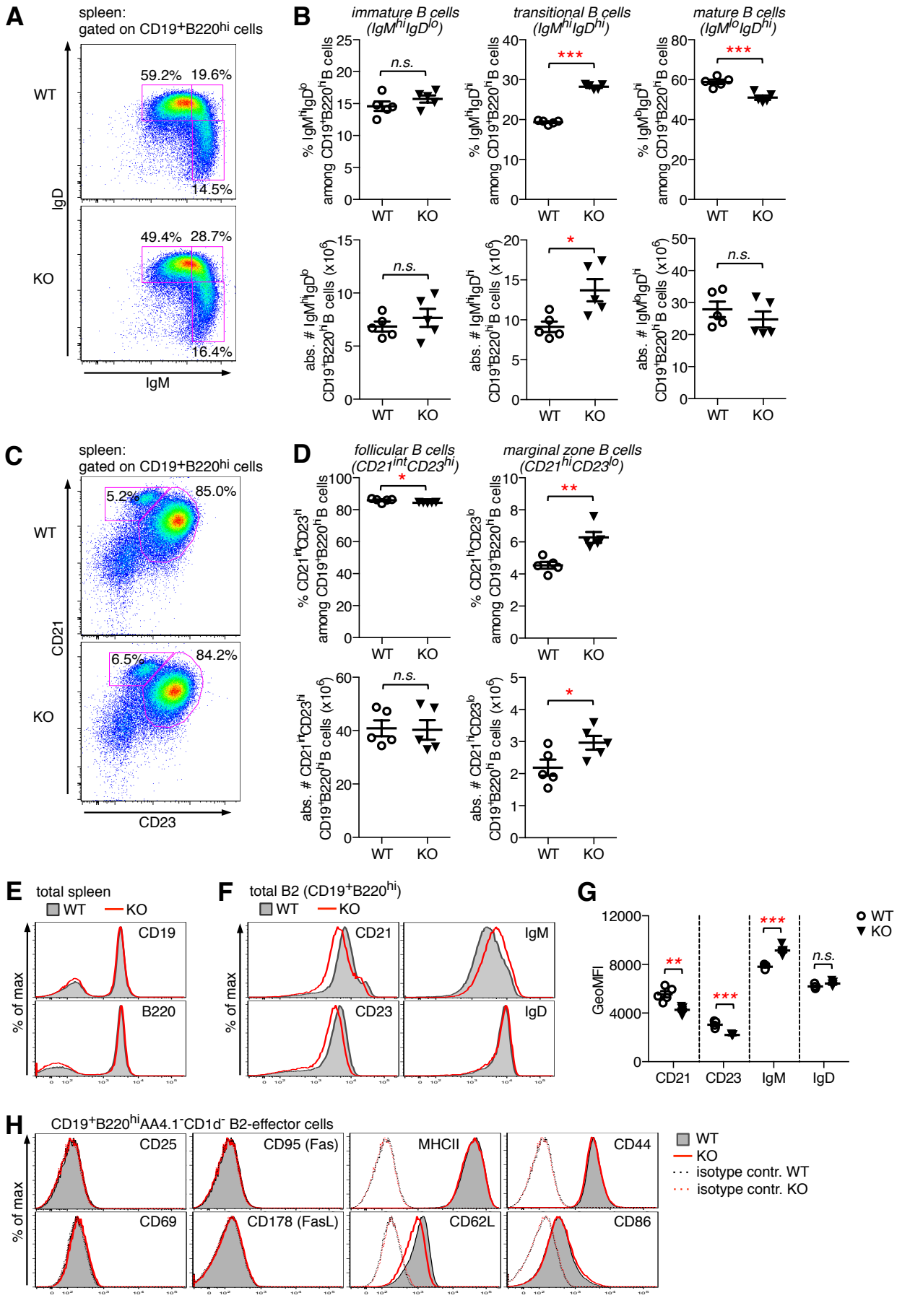

Yu et al., Supplemental Figure 12

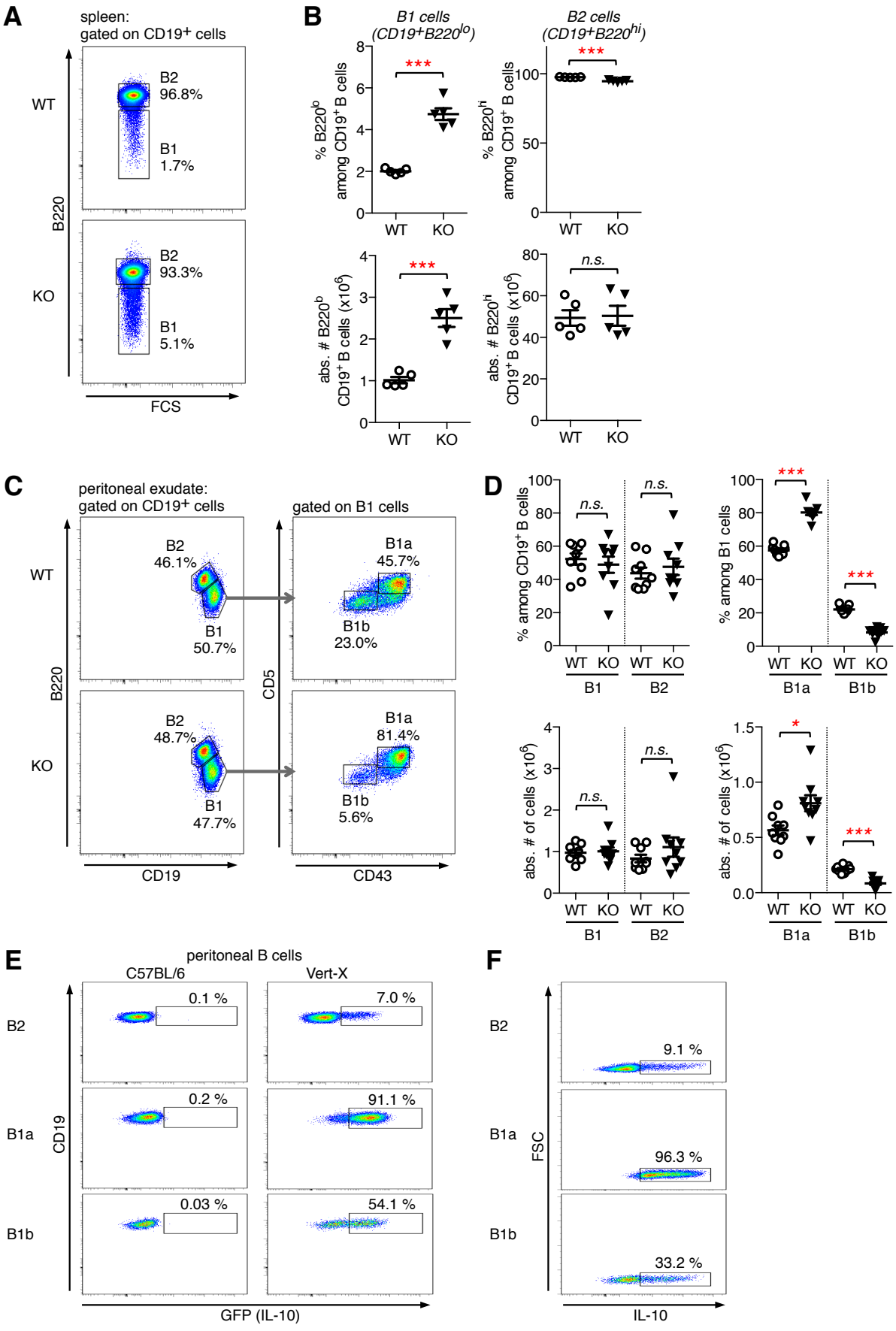

Yu et al., Supplemental Figure 13

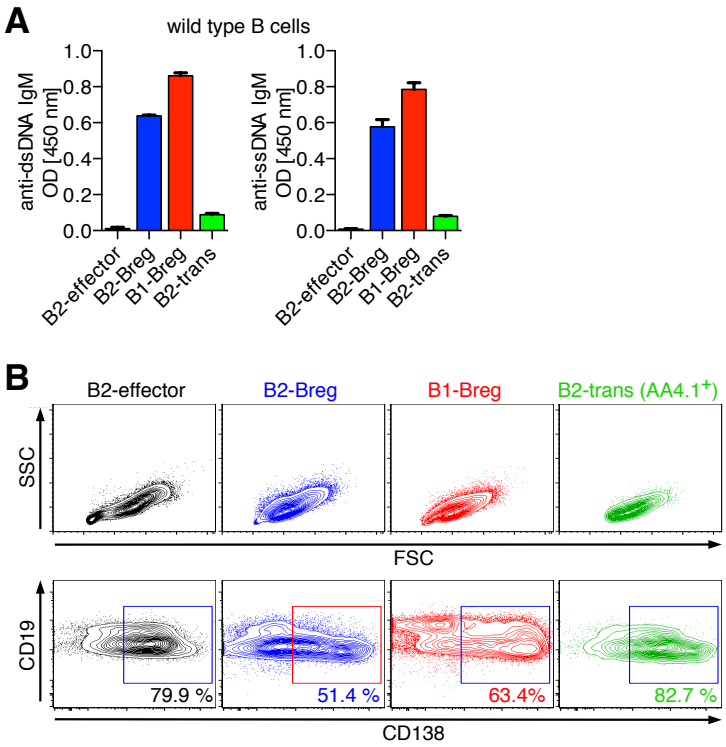
A
wild type B cells
anti-dsDNA IgM OD [450 nm]
anti-ssDNA IgM OD [450 nm]
1.0
0.8
0.6
0.4
0.2
0.0
B2-effector
B2-Breg
B1-Breg
B2-trans
B
B2-effector
B2-Breg
B1-Breg
B2-trans (AA4.1+)
SSC
FSC
CD19
CD138
79.9 %
51.4 %
63.4%
82.7 %

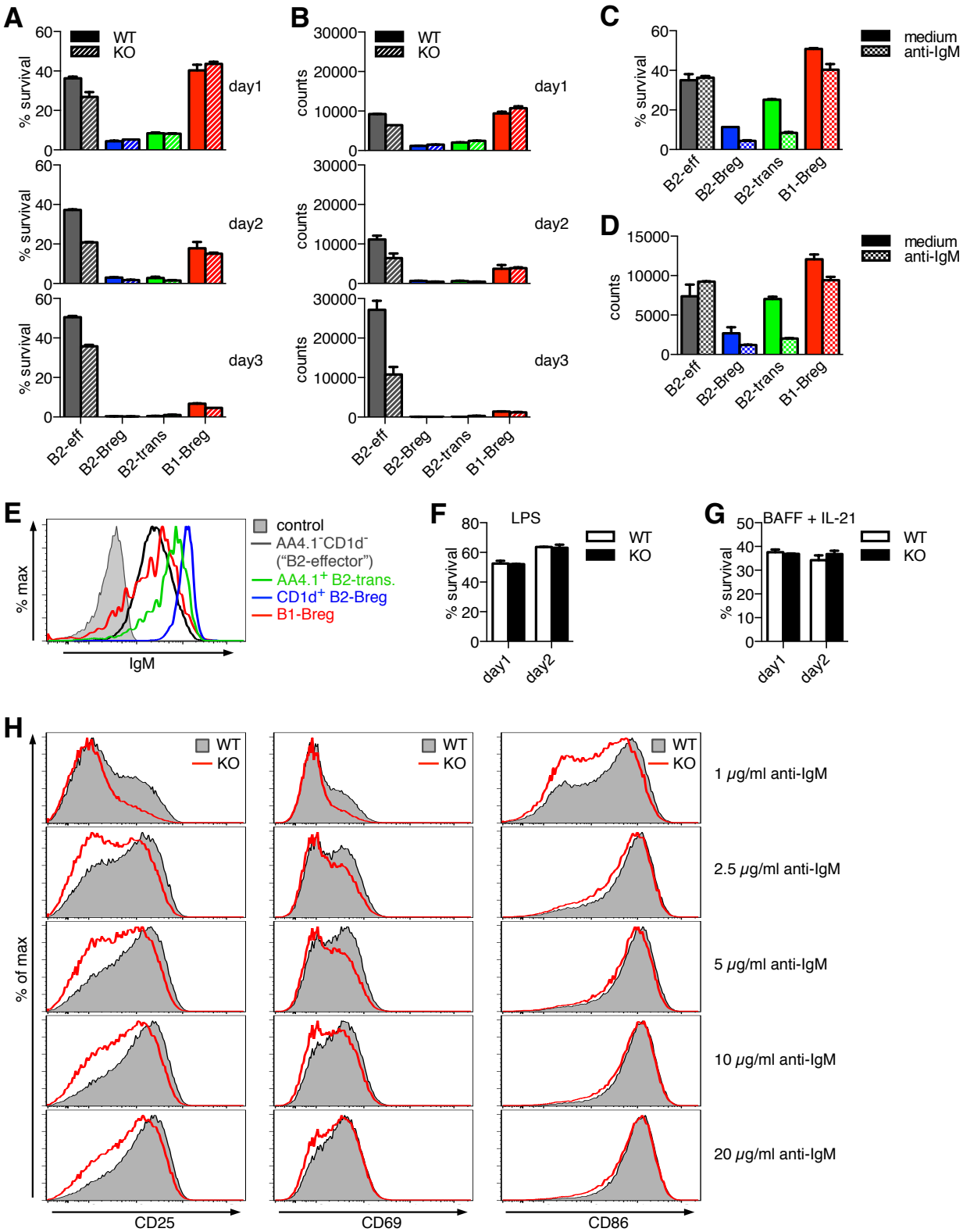
A
WT
KO
% survival
day1
day2
day3
B2-eff
B2-Breg
B2-trans
B1-Breg
B
counts
C
medium
anti-IgM
D
E
control
AA4.1⁻CD1d⁻
("B2-effector")
AA4.1⁺ B2-trans.
CD1d⁺ B2-Breg
B1-Breg
% max
IgM
F
LPS
G
BAFF + IL-21
H
1 μg/ml anti-IgM
2.5 μg/ml anti-IgM
5 μg/ml anti-IgM
10 μg/ml anti-IgM
20 μg/ml anti-IgM
% of max
CD25
CD69
CD86

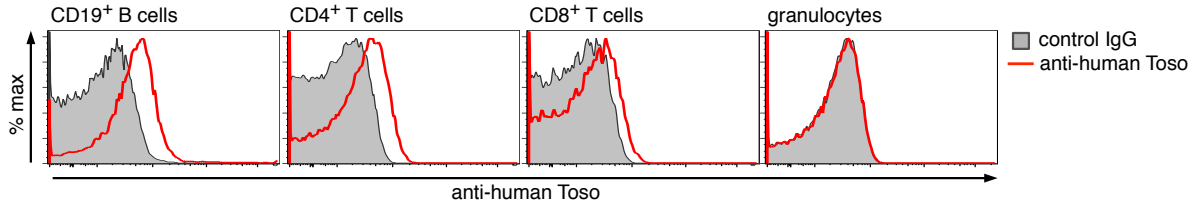

Yu et al., Supplemental Figure 16

A *wild type:*

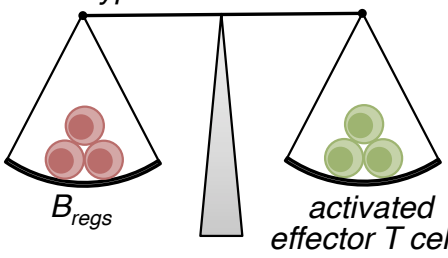

balanced system:
normal T cell immunity

B *Toso.knock-out:*

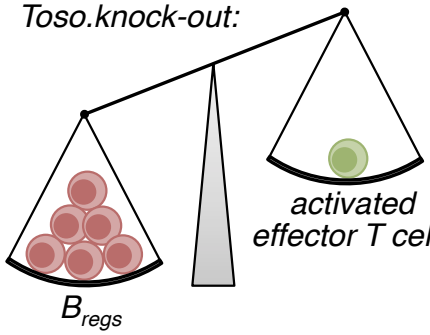

dysregulated system:
suppressed T cell immunity

- *acute viral infection:*
  impaired protective T cell response
- *chronic inflammatory disorder:*
  reduced T cell-mediated immunopathology

C

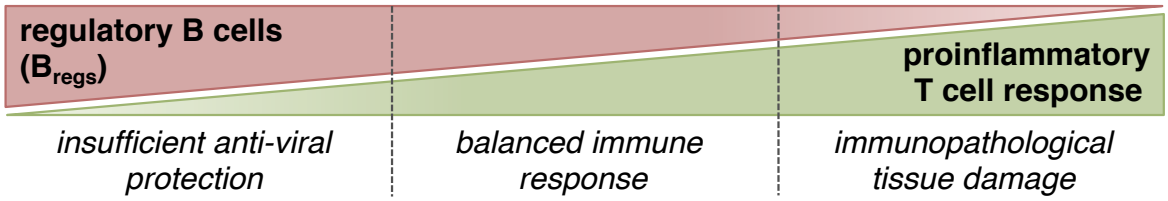

Supplemental Table 1

Description of fluorescent-labeled antibodies used in the study:

antibody specificity	clone	fluorophore(s)	source
CD1d	1B1	FITC, PE, APC, PerCPCy5.5	Biolegend
CD4	GK1.5	Brilliant Violet 510, PerCPCy5.5, Fitc	Biolegend
CD5	53-7.3	APC, PerCPCy5.5	Biolegend
CD8a	53-6.7	Brilliant Violet 510, PerCPCy5.5, PE	Biolegend
CD19	6D5	Brilliant Violet 510	Biolegend
CD21/CD35	7E9	Alexa488, PerCPCy5.5, APC	Biolegend
CD23	B3B4	PE	eBioscience
CD25	PC61.5	PE, APC	eBioscience
CD43	R2/60	PE, APC	eBioscience
CD44	IM7	Fitc, PE, APC	Biolegend
CD62L	MEL-14	PE, APC	Biolegend
CD69	H1.2F3	Alexa488, APC	Biolegend
CD73	TY/11.8	PE, APC	Biolegend
CD80	16-10A1	PE, APC	Biolegend
CD86	GL-1	PE, APC	Biolegend
CD93	AA4.1	PE, APC	Biolegend
CD95 (Fas)	15A7	Alexa488, PE	eBioscience
CD178 (FasL)	MFL3	PE, APC	Biolegend
CD138	281-2	PE, APC	Biolegend
CD178	MFL3	PE, APC	eBioscience
B220	RA3-6B2	Brilliant Violet 510, PerCPCy5.5, APC	Biolegend
F4/80	BM8	PerCPCy5.5, Alexa 488, APC	eBioscience
GL7	GL7	PE	eBioscience
IgD	11-26c.2a	Alexa 488, APC	Biolegend
IgM	RMM-1	PE, APC, PerCPCy5.5	eBioscience
MHCII	M5/114.15.2	PE	Biolegend
NK1.1	PK136	PerCPCy5.5, Alexa 488, APC	Biolegend
PD-1	J43	PE, APC	eBioscience
PD-L2	112	PE, APC	eBioscience
Tim-1	RMT1-4	PE	Biolegend
TNFα	MP6-XT22	Alexa 488, APC	Biolegend
IFNγ	XMG1.2	PE, APC	Biolegend
IL-10	JES5-16E3	PE, APC	Biolegend